24. SEQUENCE EFFECTS IN FATIGUE CRACK GROWTH DESCRIBED ON A CONTINUUM MECHANICS BASIS

H. Führing [1] and T. Seeger [2]

When regarding constant amplitude (C.A.) loading as the simplest type of cyclic loading (Fig. 1) common knowledge is that crack growth is a continuous process with an unequivocal law - for fixed environmental conditions depending mainly upon the effective stress intensity range, ΔK_{eff}, due to the load range above the crack opening level. The hope was that any kind of irregular loading could be interpreted as a series of C.A. cycles of varying magnitude. Crack length would then be the sum of these C.A. crack growth increments. Unfortunately, that is not the case. Cracks seem to grow as they want to do.

In the authors' opinion the crack growth law is valid furtheron. However, the real ΔK_{eff} development differs from that which would have been expected from considering the single cycles. ΔK_{eff} is governed by a kind of structural memory of the preceeding load cycles. With other words: The rate of cyclic crack growth depends upon load sequence effects / 1 / which are due to the elasto-plastic response of materials / 2 /.

Two of the most typical load sequence effects are schematically depicted in Fig. 2. First, due to the jump from low to high loading this sequence shows accelerated crack growth. "Accelerated" means that the actual crack growth is faster than that of pure high load cycling without the preceeding low cycles. Second, the load returning to the previous load level causes retarded crack growth - what means that the actual crack growth can be much slower than the crack growth under pure low load cycling. How much depends upon the height of the load jump and some other parameters. The schematic drawing gives the additional information that the life increasing retardation effect generally is one order of magnitude greater than the corresponding acceleration effect.

1) Laboratorium für Betriebsfestigkeit (LBF), Darmstadt, der Fraunhofer-Gesellschaft

2) Technical University of Darmstadt, Germany

Each irregular load-time function should be resolvable into discrete occurences of a few basic load sequences with known crack growth behaviour so that we are able to make realistic life predictions of structural components under service conditions.

Following this concept, in the past the authors investigated crack growth by means of the Fatigue Fracture Mechanics theory / 3, 4 / and reported on computations of the elasto-plastic stress-strain field at a crack tip from load reversal to load reversal. The case studies brought insight into the continuumechanics background of the fatigue crack growth process which is mainly governed by crack closure. The need at the present is to find out what are the independent variables of the load sequence effects and what are the pure material parameters. In the present paper a rough approach to only one of several load sequence problems is tried. In order to make the results translucable it is based on some engineering assumptions rather than on more accurate crack closure solutions.

We restrict ourselves to the special case named "Single Peak Overloading" including a possible subsequent peak underload. Its typical crack growth curve is depicted on the right hand side of Fig. 3, the first derivation, i.e. the crack growth rate, on the left hand side. Where the sequence or load interaction effect ceases- that is where the actual crack growth rate reaches C.A. values - there is the point at which the delay or retardation effect can be quantified. The total number of affected cycles N_{SP} is split up into the number of cycles N_{CA} which would have been obtained without the peak load, plus the so-called number of delay cycles N_D / 5 /. N_{SP} and N_D shall be the descriptive quantities for the single peak overload response of the material. To formulate their dependence on the load sequence and the material parameters is the intention of the paper.

With Fig. 4 the field of phenomenogical considerations is left. You find compared the Fatigue Fracture Mechanics model / 4 / on the left hand side and on the right hand side the simplified model used here for establishing an approximate closed solution. The da/dN plot was rotated to the more common kind of representation with the crack length on the abscissa.

The refined theory / 4 / models the real behavior in thin sheets fairly well. Individual examples of the problem group concerned can be solved with this tool. However, it must be said that this way is too complicated for general use. In the figure you find the size-development of the plastic zone with crack length increase and the ΔK_{eff}-development which corresponds to the da/dN development the typical behaviour of which is in accordance with the experimental findings. Though, actually, theory / 2 / and most experiments (e.g. / 6 /) indicate that the interaction is not yet finished when the plastic zone strikes the peak-load-induced elasto-plastic boundary, the simplified model works with this endpoint. This deviation can be proved to have a minor influence on the model accuracy. A further simplication concerns the ΔK_{eff}-function which we assume to consist of two straight lines to and from the minimum. This was done to achieve a simple closed integration.

The relationship for N_{SP} shown in Fig. 5 is derived by means of the crack growth law [1] and the simplified ΔK_{eff} function. When analyzing the integral solution we observe that the second term guided by Δa_M can be neglected since, compared to the first term, it inherits the product of two small quantities.

As a result the total number of cycles is a function of the exponent of the C.A. crack growth law, a function of Δa_D which can be easily calculated, and of γ_D which is the ratio of two ΔK_{eff} values. Equivalently, γ_D can be written as the ratio of the stabilized crack growth rate to the minimum crack growth rate. The problem, however, is not yet solved as the minimum growth rate value still is an unknown quantity.

But the formula indicates the governing character of the minimum crack growth rate for the load sequence effect. This minimum is a important as the length of the interaction zone, Δa_D. Thanks to the publication of min da/dN data in two references / 7, 8 / we are in a position to corroborate this finding before going forth. In Fig. 6 experimentally found numbers of overload affected cycles are depicted in a normalized manner versus the respective values of γ obtained from the published minimum da/dN values. The normalization is made with the number

[1] $da/dN = C \cdot \Delta K_{eff}^{\;m}$

of C.A. cycles for the same increase in crack length. The materials are a mild steel and aluminum 2024 both with an exponent of $m = 3$, approximately. The associated theoretical curve runs in the midth of the experimental results. The outer lines are the factor of two lines with respect to the relative cycle number.

With this encouraging proof in mind we continue to seek for a closed solution where the minimum crack growth rate can be expressed through known parameter values. Fig. 7 demonstrates the way of thinking based on the findings of the Fatigue Fracture Mechanics studies / 4 /. They revealed that the development of the plastic zone size with crack growth - see the lower right hand corner - is quite similar to the ΔK_{eff} development. The respective two minima just occur when the plastic zone strikes the compressive plastic zone of the peak cycle / 3 /.
As, under SSY assumptions, ΔK_{eff} is found to be proportional to the square root of the plastic zone size ω, which holds even for the sequence effect considered here, the crack growth rate minimum, too, must be a power function of the minimum plastic zone size. The proportionality factor can be obtained by fulfilling the limit condition with no overload. Hence, by inserting the closed SSY solution for the ω-minimum

$$\omega_M = \frac{\pi}{8}\left(\frac{\Delta K_S}{2\sigma_y}\right)^2 \cdot \left(P^* - P\right)^2 \qquad \Delta K_S = K_S - K_i$$

into γ of the integral solution

$$\gamma \equiv \frac{(da/dN)_D}{(da/dN)_M} = \left(\frac{P^* - 1}{P^* - P}\right)^m$$

the final formula is obtained. The intermediate steps of the derivation can be made straight forwardly by using the solution, the authors presented at the ASTM Fracture Symposium / 9 /.

The one point to feature out is, that the plastic zone size minimum is a function of what the authors call the "peak cycle ratio P", defined in the upper right hand corner of Fig. 7. This P-ratio turns out to be the independent variable in the relationship for the N_{SP} / N_{CA} - ratio.

The final formula is written down in the upper left hand corner of Fig. 8.
P^* and τ have theoretically known values: $P^* = 2$, $\tau = m - 1$.
Since, however, the real material behaviour could not be correctly modelled by the approach, these two quantities were taken as free constants. P^* is that value of P where crack arrest i.e. infinite crack growth life can be observed. Theoretically, it occurs if P equals 2 what, in case of $R = 0$, means a hundred percent overload with no underload. However, experimental values lie between the values of 2 and 3. If there exists a material characteristic curve where the ratio N_{SP} / N_{CA} is only a function of the P-ratio and the two material constants one straightforwardly gets the desired number of delay cycles for any load values considered.

Instead of only two references available for the first proof of the theoretical approach we can now use results of approximately five hundred experiments on six materials by twelve authors / 5, 10 – 20 /. Only few of them are shown in the figures.

A difficulty arose from the fact that mostly no constant amplitude data of the tested materials were published (cf. the suggestion in / 21 /). They had to be estimated. This fact must be taken into consideration when judging on the scatter of results. The symbols in Figures 9 and 10 represent the experimentally evaluated N_{SP} / N_{CA} ratio versus the peak range ratio of the load sequence applied. You also see the theoretical curve with the values which seem to fit the experimental data best. The comparison of the Aluminum to the Titanium data yields less delay for the Titanium. The exponents differ whereas the crack arrest ratio is identical for both materials.

On the left hand side of Fig. 10 the experimental results for three different steels are compared to the theoretical curve with the indicated parameter values. On the right hand side one test group was analyzed with respect to the occurence frequency. Only five of fiftyfive values lie outside the factor of 2 limits. These are mostly long life data with P values greater than 2 where the scatterband in cycles loses its usefulness.

Fig. 11 gives some examples on the predictions which can be made with this instrument. Each new combination of load values, crack length, specimen geometry and loading case, confronts you again with the question: What is the effect on life? With the presented formula this can be answered to a certain extent.
To summarize the central idea of the paper:
The functional type of a relationship is presented describing single peak overload delay cycles as a function of a sole parameter. The absolute number of delay cycles depends on the C.A. crack growth behaviour of the material and at least two material constants. Those material constants must be evaluated from experiments. It is a first attempt to find the basic scheme behind this class of load sequences. Such a procedure would be promising also for other typical cases of load sequences. Valuable experiments are already carried out on this field but a similar interconnection between theory and experiment is not yet found. The present relationships are derived on the basis of elasto-plastic Fatigue Fracture Mechanics solutions including crack closure but with some very simplifying assumptions.

The authors wish to acknowledge the support given by the Deutsche Forschungsgemeinschaft (DFG) for important parts of this investigation.

REFERENCES

[1] Schijve, J.:
The Accumulation Fatigue Damage in Aircraft Materials and Structures
AGARDograph No. 157, 1972.

[2] Führing, H.; Seeger, T.:
Acceleration and Retardation Effects with Fatigue Crack Growth and their Calculation Based on Fatigue Fracture Mechanics
Second International Conference on Mechanical Behavior of Materials, Boston, 1976, S. 721-725.

[3] Führing, H.; Seeger, T.:
Remarks on Load-Interaction Effects Based on Fatigue Fracture Mechanics Calculations
Proceedings of the Ninth ICAF Symposium on Aeronautical Fatigue, Darmstadt, 1977, S. 5.3/1-12.

[4] Führing, H.:
Berechnung von elastisch-plastischen Beanspruchungsabläufen in Dugdale-Rißscheiben mit Rißuferkontakt auf der Grundlage nichtlinearer Schwingbruchmechanik
Veröffentlichungen des Instituts für Statik und Stahlbau, Technische Hochschule Darmstadt, Heft 30, 1977, 256 Seiten.

[5] Schijve, J.:
Fatigue Damage Accumulation and Incompatible Crack Front Orientation
Engineering Fracture Mechanics, 1974, S. 245-252.

[6] van Lipzig, H.T.M.; Nowack, H.:
Rißfortschrittsverhalten und Restfestigkeit von Leichtbauwerkstoffen bei nicht-einstufigen Belastungen
DVM, 6. Sitzung Bruchvorgänge, Freiburg, 1974, S.129-141.

[7] Seeger, T.; Hanel, J.J.:
Der Einfluss von plastischen Verformungen sowie von last- und temperaturinduzierten Eigenspannungen auf das Dauerfestigkeitsverhalten von Kerb- und Risstäben.
In: VDI-Berichte 268, VDI-Verlag Düsseldorf, 1976, S.77-92.

[8] Alzos, W.X., Skat, A.C.; Hillberry, B.M.:
Single Overload/Underload Cycles on Fatigue Crack Propagation
In: ASTM-STP 595, 1976, S. 41-60.

[9] Führing, H.; Seeger, T.:
Structural Memory of Cracked Components Under Irregular Loading
To appear in: ASTM STP (11th Symposium on Fracture Mechanics 1978).

[10] Mills, W.J.:
Load Interaction Effects on Fatigue Crack Growth in 2024-T 3 Aluminum and A 514 F Steel Alloys
Department of Metallurgy and Materials Science, Lehigh University, Bethlehem, 1975.

[11] Rice, R.C.; Stephens, R.I.:
Overload Effects on Subcritical Crack Growth in Austenitic Manganese Steel. In: ASTM-STP 536, 1973, S. 95-114.

[12] Stephens, R.I.; Chen, D.K.; Hom, B.W.:
Fatigue Crack Growth with Negative Stress Ratio Following Single Overloads in 2024-T 3 and 7075 - T 6 Aluminum Alloys. In: ASTM STP 595, 1976, S. 27-40.

[13] Stephens, R.I.; McBurney, G.W.; Oliphant, L.J.:
Fatigue Crack Growth with Negative R-Ratio Following Tensile Overloads.
Int. Journ. of Fracture 10, 1974, S. 587-589.

[14] Himmelein, M.K.; Hillberry, B.M.:
Effect of Stress Ratio and Overload Ratio on Fatigue Crack Delay and Arrest Behaviour Due to Single Peak Overloads
In: ASTM-STP 590, 1976, S. 321-330.

[15] Probst, E.P., Hillberry, B.M.:
Journal, American Institute of Aeronautics and Astronautics, 12, 1974. S. 330.

[16] Trebules Jr., V.W.; Roberts, R.; Hertzberg, R.W.:
Effect of Multiple Overloads on Fatigue Crack Propagation in 2024-T 3 Aluminum Alloys
In: ASTM-STP 536, 1973, S. 115-146.

[17] Von Euw, E.F.J.; Hertzberg, R.W.; Roberts, R.:
Delay Effects in Fatigue Crack Propagation
In: ASTM-STP 513, 1972, S. 230-259.

[18] Shih, T.T.; Wei, R.P.:
A Study of Crack Closure in Fatigue
Engineering Fracture Mechanics, Vol. 6, 1974. S. 19-32.

[19] Wei, R.P.; Shih, T.T.:
Delay in Fatigue Crack Growth
Int. Journ. of Fracture, 10, 1974, S. 77-85.

[20] Chanani, G.R.:
Fundamental Investigation of Fatigue Crack Growth Retardation in Aluminum Alloys
AFML-TR-76-156, 1976, Northrop Corp., Hawthorne, Ca.

[21] Führing, H.; Seeger, T.:
A Suggestion for Systematic Load Interaction Studies on Fatigue Crack Growth
Int. Journal of Fracture 12, 1976, S. 307-310.

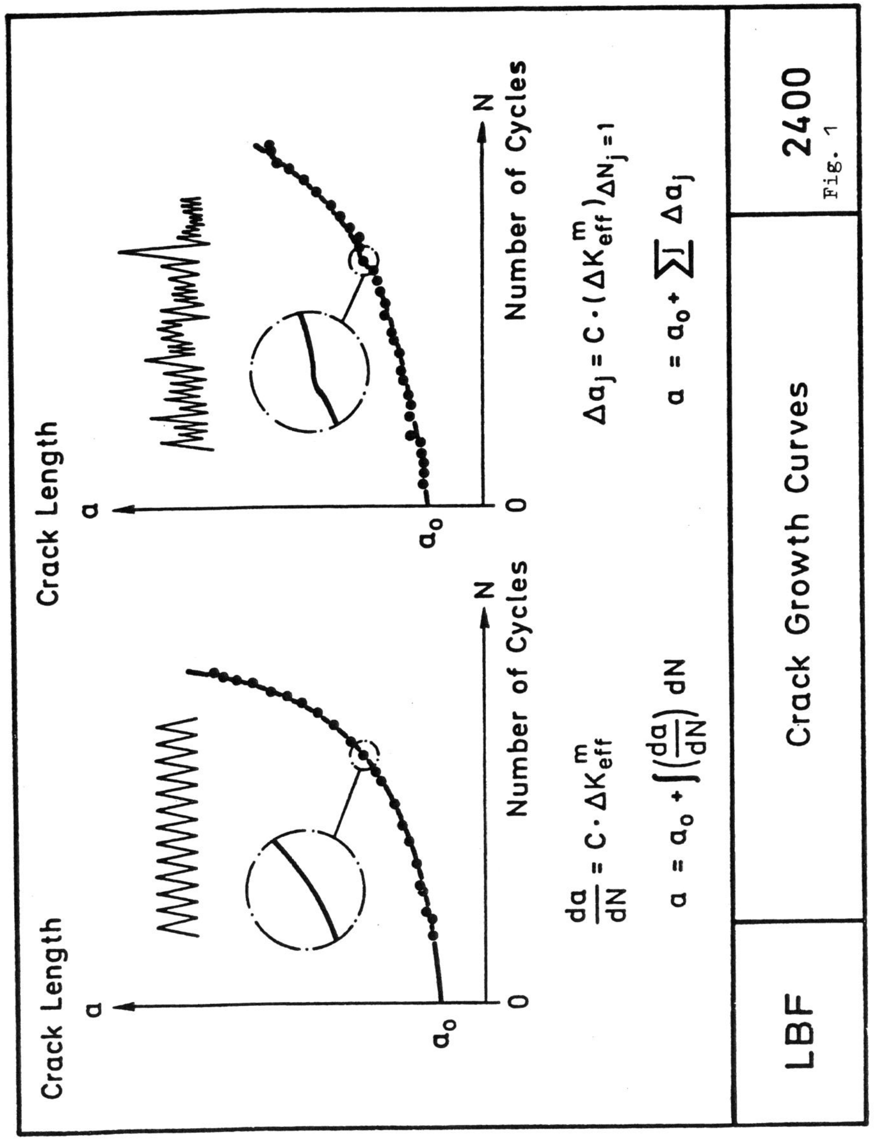
Crack Length
a
a_o
0
N
Number of Cycles
$\frac{da}{dN} = C \cdot \Delta K_{eff}^m$
$a = a_o + \int \left(\frac{da}{dN}\right) dN$
Crack Length
a
a_o
0
N
Number of Cycles
$\Delta a_j = C \cdot (\Delta K_{eff}^m)_{\Delta N_j = 1}$
$a = a_o + \sum \Delta a_j$
LBF
Crack Growth Curves
2400
Fig. 1

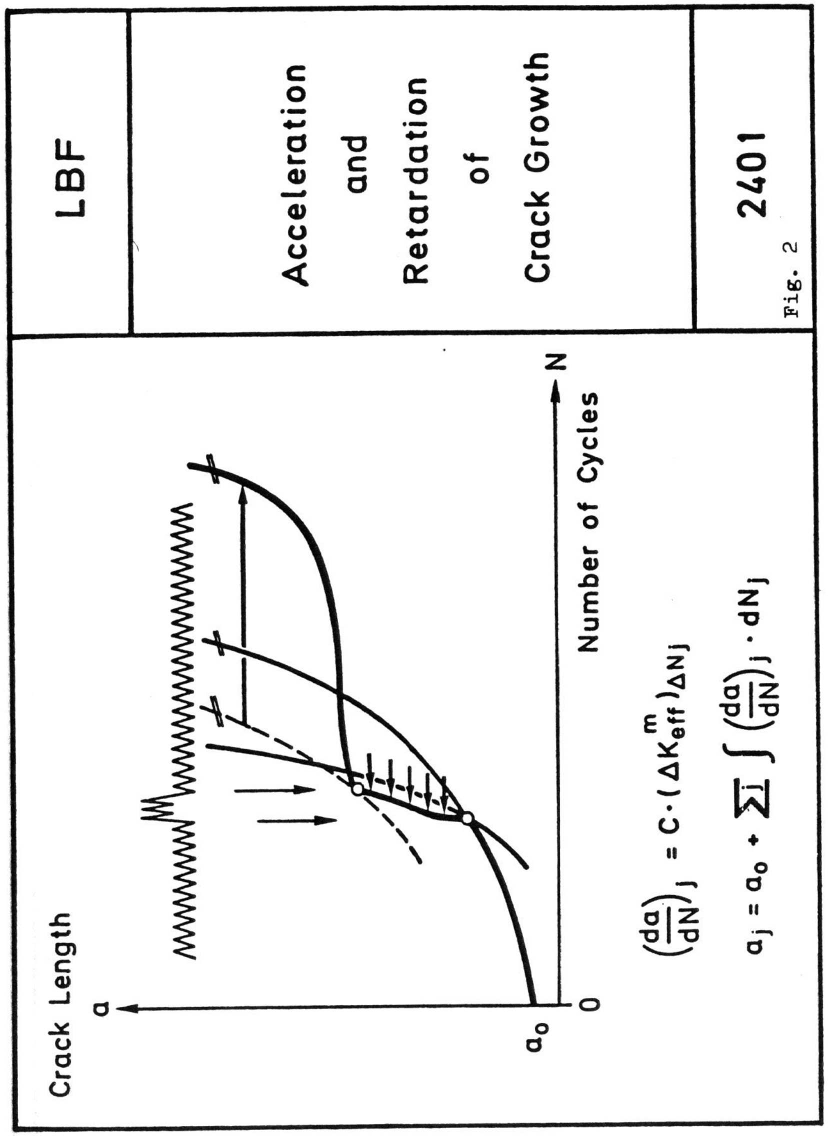
LBF
Acceleration
and
Retardation
of
Crack Growth
2401
Fig. 2
Crack Length
a
a_o
0
N
Number of Cycles
$\left(\frac{da}{dN}\right)_j = C \cdot (\Delta K_{eff}^m)_{\Delta N_j}$
$a_j = a_o + \sum_j \int \left(\frac{da}{dN}\right)_j \cdot dN_j$

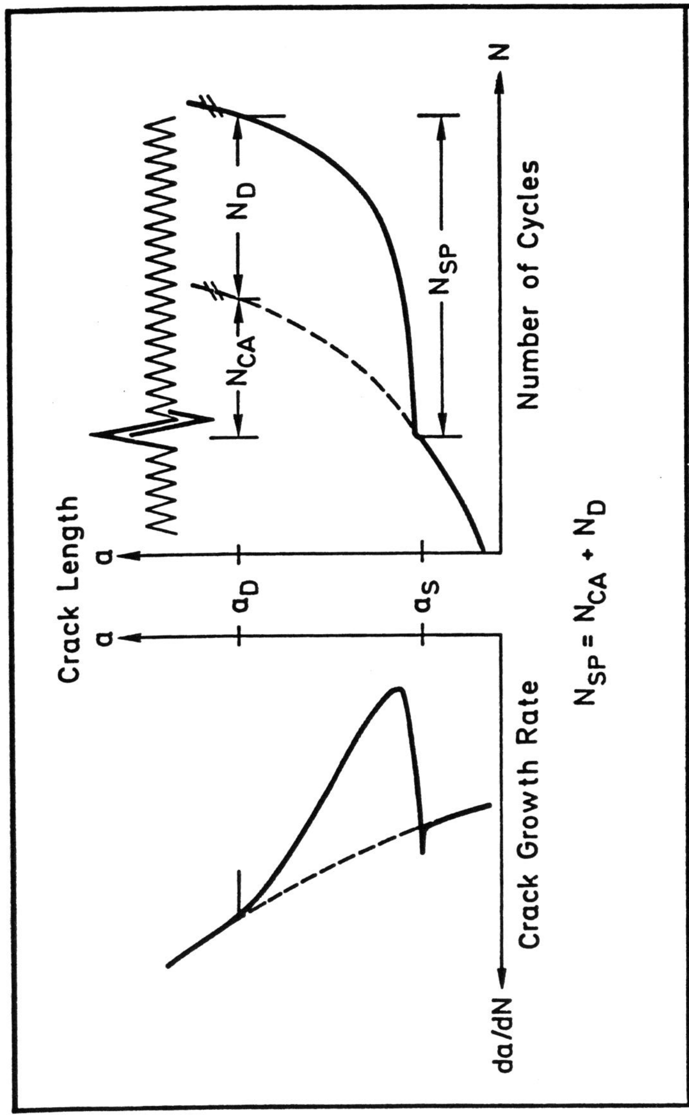

LBF | Single Peak Overload | 2402 Fig. 3

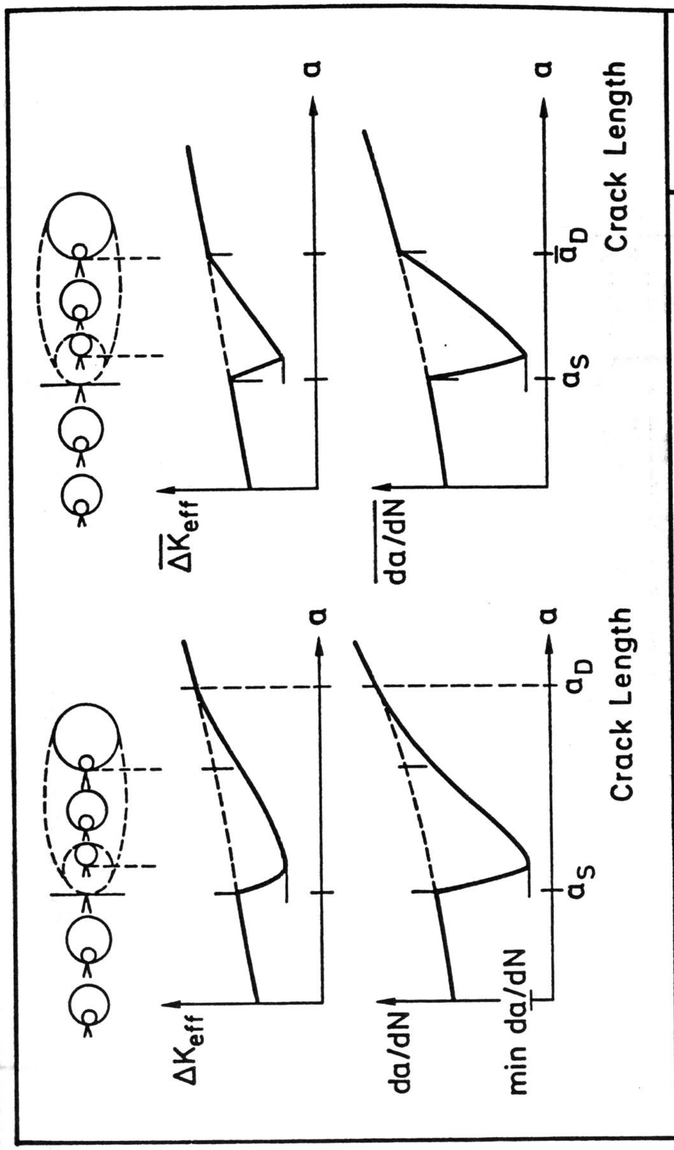

LBF | Fatigue Fracture Mechanics and Simplified Model | 2403 Fig. 4

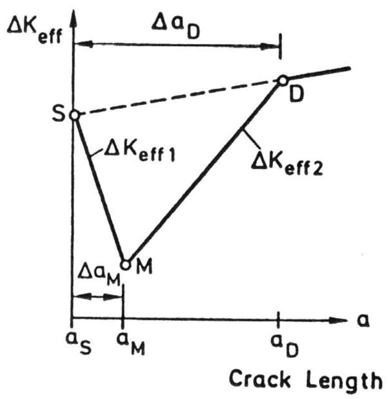

$$N_{SP} = \int_{a_S}^{a_D} \frac{da}{(da/dN)} = \frac{1}{C}\left[\int_{a_S}^{a_M} \frac{da}{\Delta K_{eff1}^{m}} + \int_{a_M}^{a_D} \frac{da}{\Delta K_{eff2}^{m}}\right]$$

$$(m-1)\, N_{SP} = \frac{\Delta a_D}{(da/dN)_M} \cdot \frac{1-\gamma_D^{1/m-1}}{\gamma_D^{1/m}-1} + \frac{\Delta a_M}{(da/dN)_M}\left[\frac{1-\gamma_S^{1/m-1}}{\gamma_S^{1/m}-1} - \frac{1-\gamma_D^{1/m-1}}{\gamma_D^{1/m}-1}\right]$$

$$\gamma_D \equiv \left(\frac{\Delta K_{eff\,D}}{\Delta K_{eff\,M}}\right)^m = \frac{(da/dN)_D}{(da/dN)_M}$$

LBF	Functional Relationship for N_{SP}	2404 Fig. 5

Experimental Results

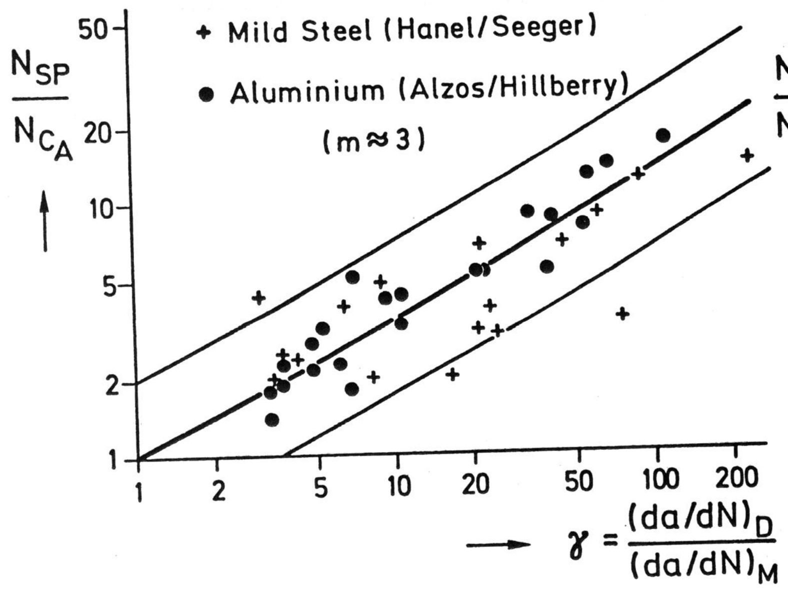

$$\frac{N_{SP}}{N_{CA}} = \frac{1}{m-1}\;\frac{\gamma_D^{1-1/m}-1}{1-\gamma_D^{-1/m}}$$

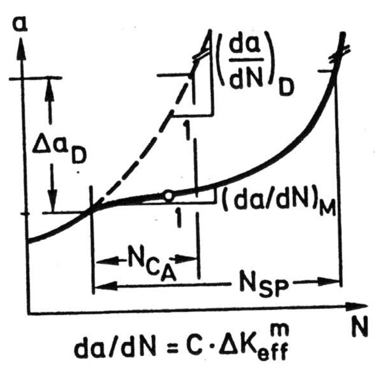

$da/dN = C \cdot \Delta K_{eff}^{m}$

LBF	Formula Verification by Experiments	2405 Fig. 6

Minimum Crack Growth Rate

$(da/dN)_M = ?$

↓

SSY-Assumption

$\Delta K_{eff} \sim \omega^{1/2}$

↓

$\left(\frac{da}{dN}\right)_M \sim \left[\omega_M^{1/2}\right]^m$

↓

Minimum Plastic Zone Size

$\omega_M = F(K_5, P, \text{Material})$

from Theory

$$P = \frac{S_3 - S_4}{S_5 - S_4}$$

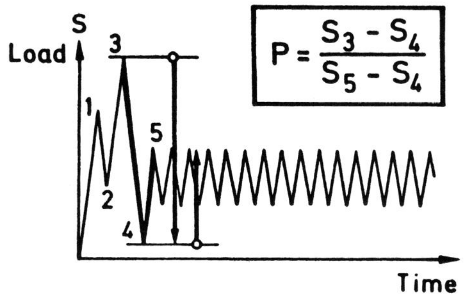

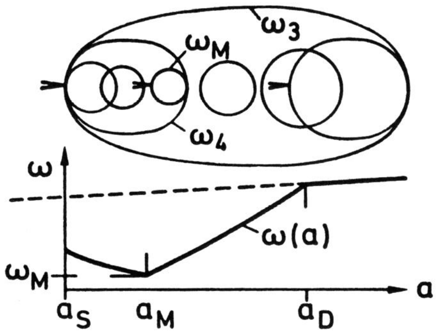

LBF | Introduction of the Peak Range Ratio P | 2406

Fig. 7

$$\frac{N_{SP}}{N_{CA}} = \frac{1}{r}\,\frac{P^*-1}{P-1}\left[\left(\frac{P^*-1}{P^*-P}\right)^r - 1\right]$$

$\left.\begin{matrix}P^* \\ r\end{matrix}\right\}$ Material Constants?

Known Values:

$$P = \frac{S_3 - S_4}{S_5 - S_4}$$

$$N_{CA} = \int^{\Delta a_D} \frac{1}{(da/dN)_{CA}}\, da$$

$$\Delta a_D = \frac{\pi}{8}\,\frac{K_3^2 - K_5^2}{\sigma y^2}$$

$$N_D = N_{SP} - N_{CA}$$

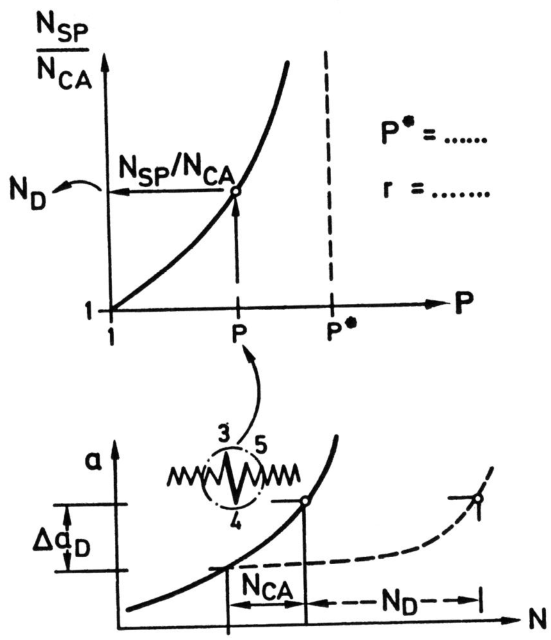

LBF | Delay Cycle Prediction | 2407

Fig. 8

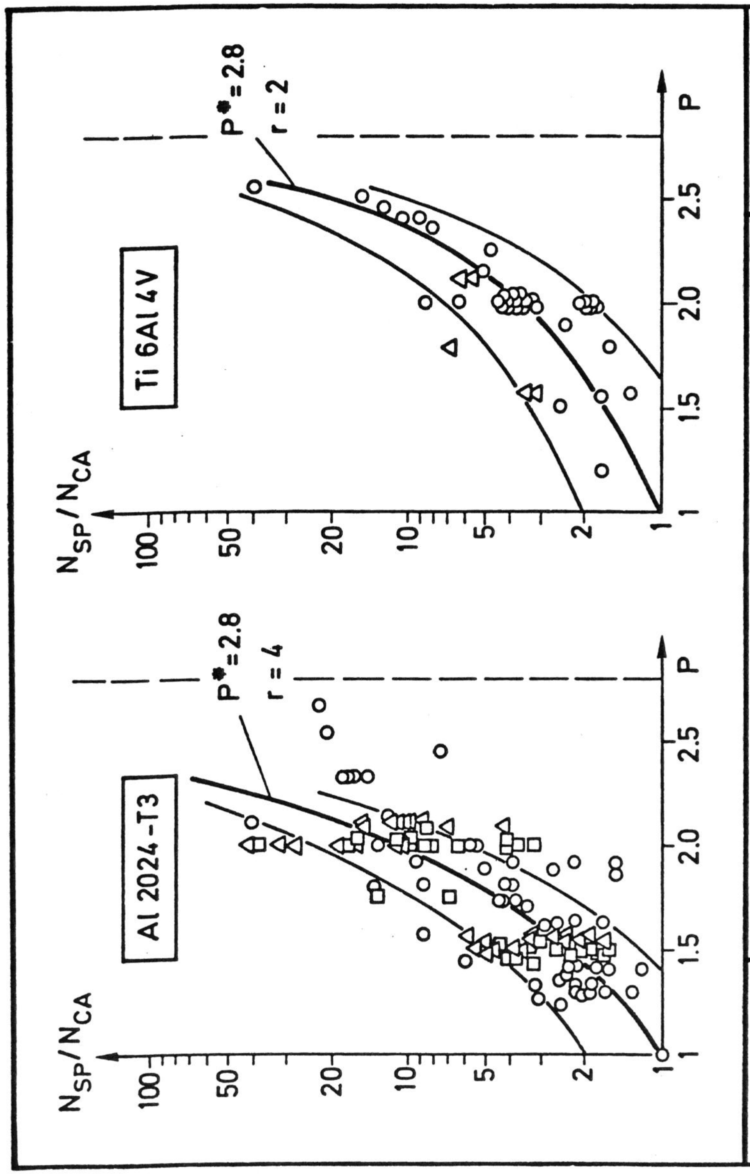

Evaluation of P* and r from Published Data

LBF

2408

Fig. 9

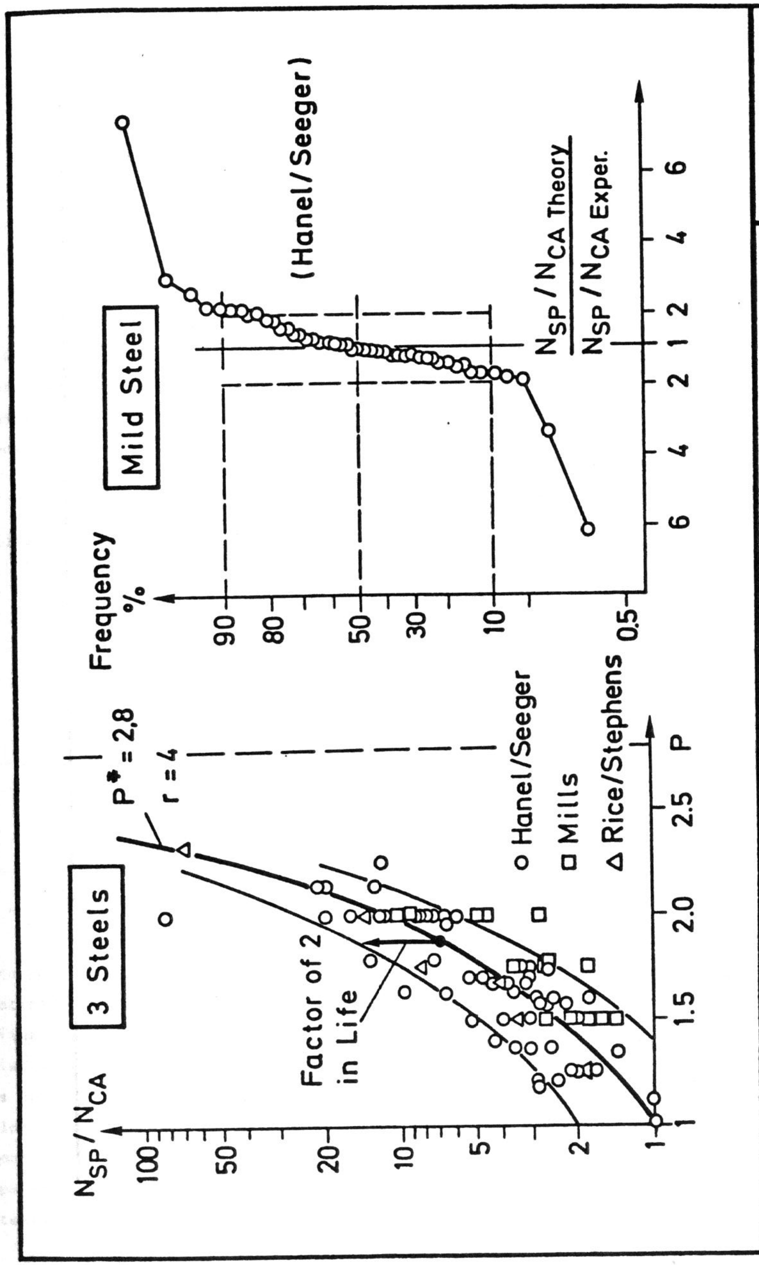

Frequence Analysis of Tests for Constants - Evaluation

LBF

2409

Fig. 10

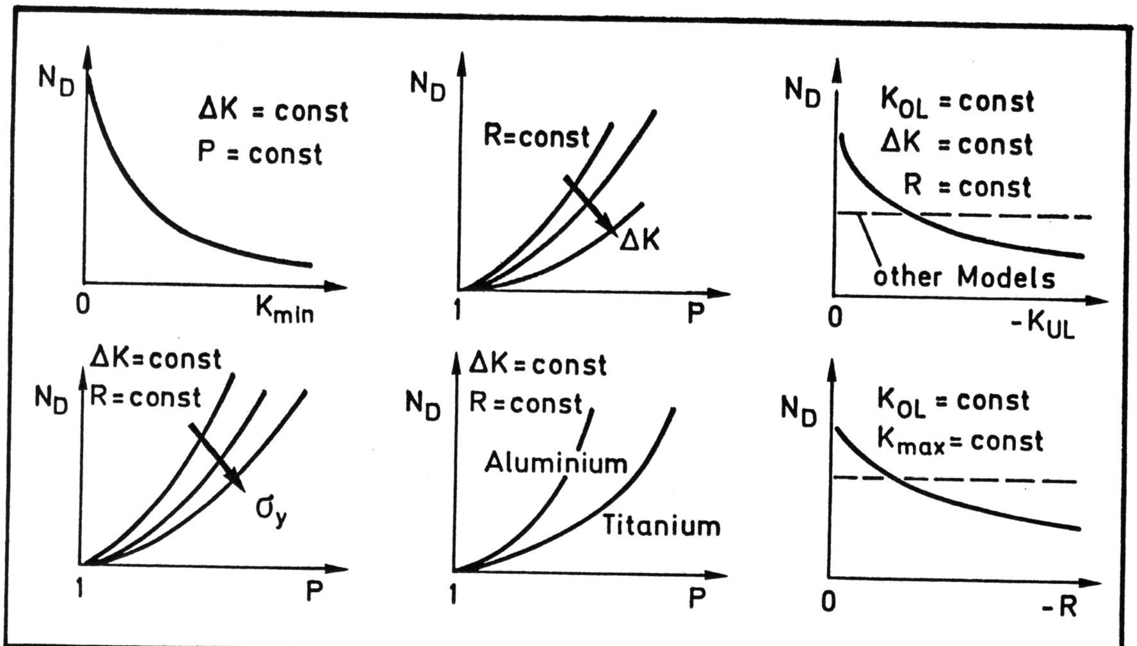

LBF	Prediction Capabilities of the Presented Formula	2410 Fig. 11